Journal of Plankton Research Vol.17 no.10 pp.1999–2008, 1995

SHORT COMMUNICATION

Changes in phytoplankton ecophysiology across a coastal upwelling front

Emilio Marañón and Emilio Fernández[1]

Departamento de Biología de Organismos y Sistemas, Unidad de Ecologia, Universidad de Oviedo, E-33071 Oviedo and [1]Departamento de Recursos Naturales y Medio Ambiente, Universidad de Vigo, Apartado 874, E-36200 Vigo, Spain

Abstract. The abundance, taxonomic composition and patterns of macromolecular synthesis of phytoplankton were determined across an upwelling-induced thermal front in the central Cantabrian Sea (southern Bay of Biscay) during July 1993. Enhanced levels of phytoplankton biomass, diatom abundance and photosynthetic rate were measured on the coastal side of the front. Relative carbon (C) incorporation into proteins increased noticeably on the oceanic side, taking values of up to 64%, whereas changes in the relative C incorporation into lipids and low-molecular-weight metabolites followed an opposite trend. Phytoplankton cells on the oceanic side of the front were adapted to the prevailing growth-limiting conditions by maintaining the synthesis of functionally essential molecules—proteins—rather than the synthesis of storage compounds. As a result, the carbon to nitrogen uptake ratio varied from ~5.7 in offshore waters to 8.0 in the nearshore region. Our results suggest that the taxonomic and physiological changes in phytoplankton assemblages as a response to upwelling may result in an increase in the synthesis of organic C relative to the upward flux of nitrate.

During coastal upwelling events, phytoplankton cells experience an increase in biomass-specific nutrient uptake rates (e.g. Wilkerson and Dugdale, 1987) and display changes in their patterns of carbon (C) allocation into different biochemical pools (e.g. Barlow, 1984). Moreover, the specific synthesis rates of proteins and polysaccharides have been proved to show up to a 5-fold increase after an advective pulse (Marañón *et al.*, 1995). These changes may partially be due to variations in the relative abundance of species (Zimmerman *et al.*, 1987). A combined approach is therefore needed where both taxonomic composition and the physiological state of phytoplankton assemblages are taken into account.

Sambrotto *et al.*, (1993) reported elevated C to nitrogen (N) consumption ratios in continental shelf regions (southeast Bering Sea and Gerlache Strait), as well as along sections in the North Atlantic, suggesting that the excess loss of dissolved inorganic C was due to biological processes that recycle N more efficiently than C. In this regard, the ^{14}C-partitioning technique is particularly useful, as it allows the estimation of phytoplankton N uptake from the measured C incorporation into the protein fraction (DiTullio and Laws, 1983). If upwelling induces a shift in the patterns of carbon partitioning among biomolecules, it may be hypothesized that phytoplankton in an upwelled water mass could show significant differences in the C:N uptake ratio as compared with microalgae in non-upwelled waters.

During July 1993, we monitored the development of a coastal upwelling pulse, taking advantage of the existence of a sharp, well-defined thermal front. We analysed the effects of upwelling on the taxonomic composition of microalgae and their patterns of macromolecular synthesis by comparing the phytoplankton

assemblages on both sides of the upwelling front. The variations in the C:N uptake ratio across the upwelling front were assessed and their potential implications for the biogeochemical cycling of C and N in upwelling systems evaluated.

Sampling was conducted in coastal and offshore waters of the central Cantabrian Sea (southern Bay of Biscay) on 13 July 1993. Fifteen surface (2–3 m depth) water samples were taken at ~1 km intervals along a transect running from 43°43.34'N, 6°09.28'W to 43°35.34'N, 6°08.77'W. In addition, the vertical distribution of the variables under study was determined at six points along the transect and at two stations located near the coastal (station A, 43°35.68'N, 6°08.60'W) and oceanic (station B, 43°42.00'N, 6°09.00'W) ends of the transect.

Surface distribution and vertical profiles of temperature and salinity were obtained with a SeaBird CTD probe. Vertical profiles of photosynthetically active radiation (400–700 nm; PAR) were determined with a Li-Cor 4π underwater sensor. Seawater samples were collected with Niskin bottles for the determination of nutrient concentration, chlorophyll *a* concentration, taxonomic composition of microplankton, and particulate organic C and N concentrations. The analytical methods followed were the same as in Fernández *et al.* (1994). Cell counts were transformed to C biomass as in Holligan *et al.* (1984). Seawater for C incorporation experiments was screened through a 200 μm sieve upon collection from the Niskin bottles. Experiments were carried out under natural light conditions in an incubator equipped with a set of neutral-density plastic screens which provided a range of irradiance levels (2, 8, 20, 40, 60 and 100% of incident irradiance). Each sample was incubated under an irradiance level similar to that experienced by the cells at the sampling depth. Temperature was kept at 17 ± 1°C by means of recirculating water. Experiments started early in the morning (~7:00 a.m.). Duplicate 70 ml polycarbonate bottles were filled with seawater from each sample, inoculated with 370 kBq (10 μCi) of $NaH^{14}CO_3$ and incubated during 24 h under a natural light–dark cycle. At the end of the incubation, samples were filtered (<100 mm Hg) through Whatman GF/F filters, which were subsequently stored at −20°C until further analysis.

The patterns of ^{14}C incorporation into different photosynthetic end-products were determined as in Fernández *et al.* (1994). This technique allows separation of cellular material into four fractions: proteins, polysaccharides and nucleic acids, lipids and low-molecular-weight metabolites (LMWM). Total carbon incorporation was calculated as the sum of the ^{14}C activity in each fraction. In previous experiments, no significant differences were found between total C incorporation in non-fractionated samples and the sum of the C incorporated into the four fractions (*t*-test, $P > 0.2$, $n = 10$). The C:N uptake ratio was calculated stoichiometrically from the percentages of ^{14}C allocation into each fraction by assuming that (i) the average molar C:N ratio is 3.8 for proteins and 3.7 for nucleic acids (Laws, 1991), (ii) the free amino acid-N to protein-N ratio was 0.05 (Dortch *et al.*, 1984), (iii) the amount of radioactive carbon present as free nucleotids was negligible (<0.5% of total incorporated carbon) and (iv) 4% of total ^{14}C fixed was incorporated into nucleic acids (Fraga and Pérez, 1990).

The vertical distribution of temperature along the transect revealed the effects of upwelling, as shown by the outcrop of isotherms towards the coast (Figure 1A).

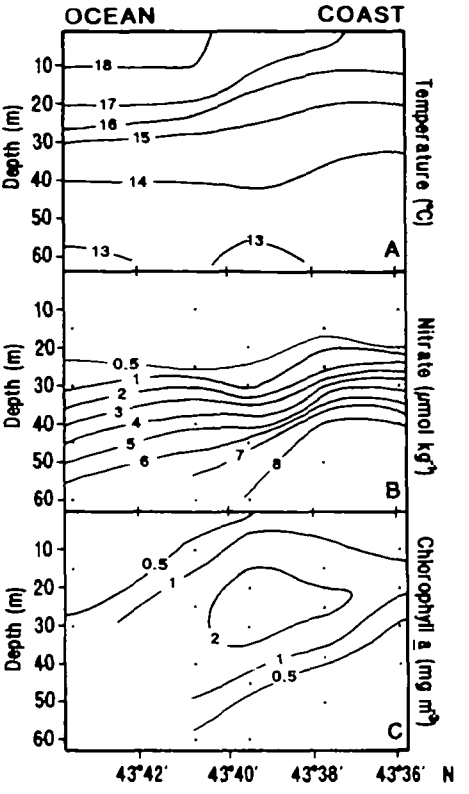

Fig. 1. Vertical distribution of (**A**) temperature (°C), (**B**) nitrate concentration (μmol kg^{-1}) and (**C**) chlorophyll *a* concentration (mg m^{-3}) along a section from 43°43.3′N, 6°09.3′W to 43°35.9′N, 6°08.8′W.

Accordingly, temperature at station A (coastal end of the transect) showed a steady decrease with depth, whereas at station B (oceanic end of the transect) a well-developed thermocline was located at 20–30 m depth (Figure 2A). Surface temperature was slightly higher than 18.2°C at stations 1–4, whereas it decreased to 16.9°C at the innermost station (station 15), thus giving rise to a thermal front with a temperature gradient of ~1.3°C over 15 km (Figure 3A).

Nitrate concentration was <0.5 μmol kg^{-1} in the upper 20–25 m throughout the transect (Figure 1B). The vertical distribution of nitrate concentration at stations A and B reflected the effects of upwelling, showing higher subsurface values at station A (Figure 2A). Surface nutrient concentrations were low throughout the transect (Figure 3A). Nitrate was undetectable at several stations on both sides of the front, taking the highest levels (~0.25 μmol kg^{-1}) at stations 8–11. Highest phosphate and silicate concentrations were found at the coastal stations. Both silicate and phosphate concentrations showed a significant inverse correlation with surface temperature ($r^2 = 0.82$, $n = 15$, $P < 0.01$). Ammonium concentrations were <0.1 μmol kg^{-1} throughout the transect (data not shown).

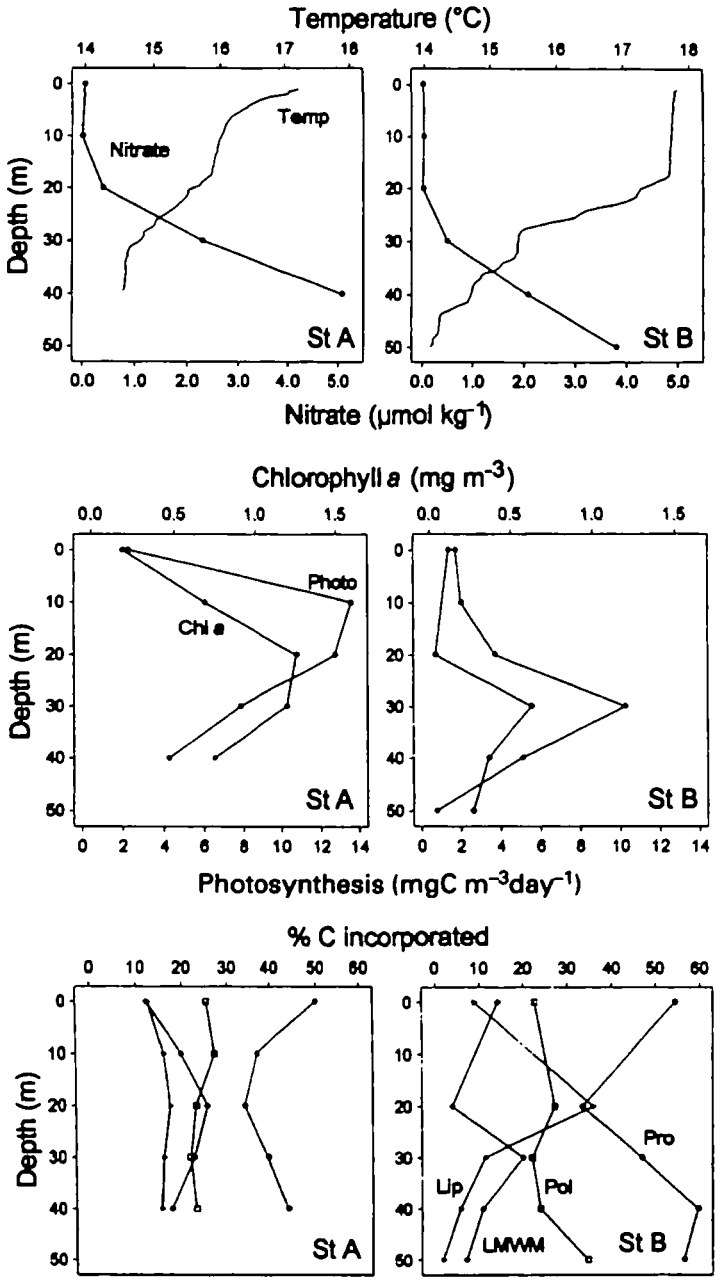

Fig. 2. Vertical profiles of (**A**) temperature (Temp, °C, ———) and nitrate concentration (µmol kg^{-1}, ○), (**B**) chlorophyll *a* concentration (Chl *a*, mg m^{-3}, ●) and total photosynthesis (Photo, mg C m^{-3} day^{-1}, ○) and (**C**) the percentage of carbon incorporation into proteins (Pro, ●), polysaccharides (Pol, □), lipids (Lip, ▲) and low-molecular-weight metabolites (LMWM, ◇) at two stations located near the coastal (station A, left panels) and oceanic (station B, right panels) ends of the transect.

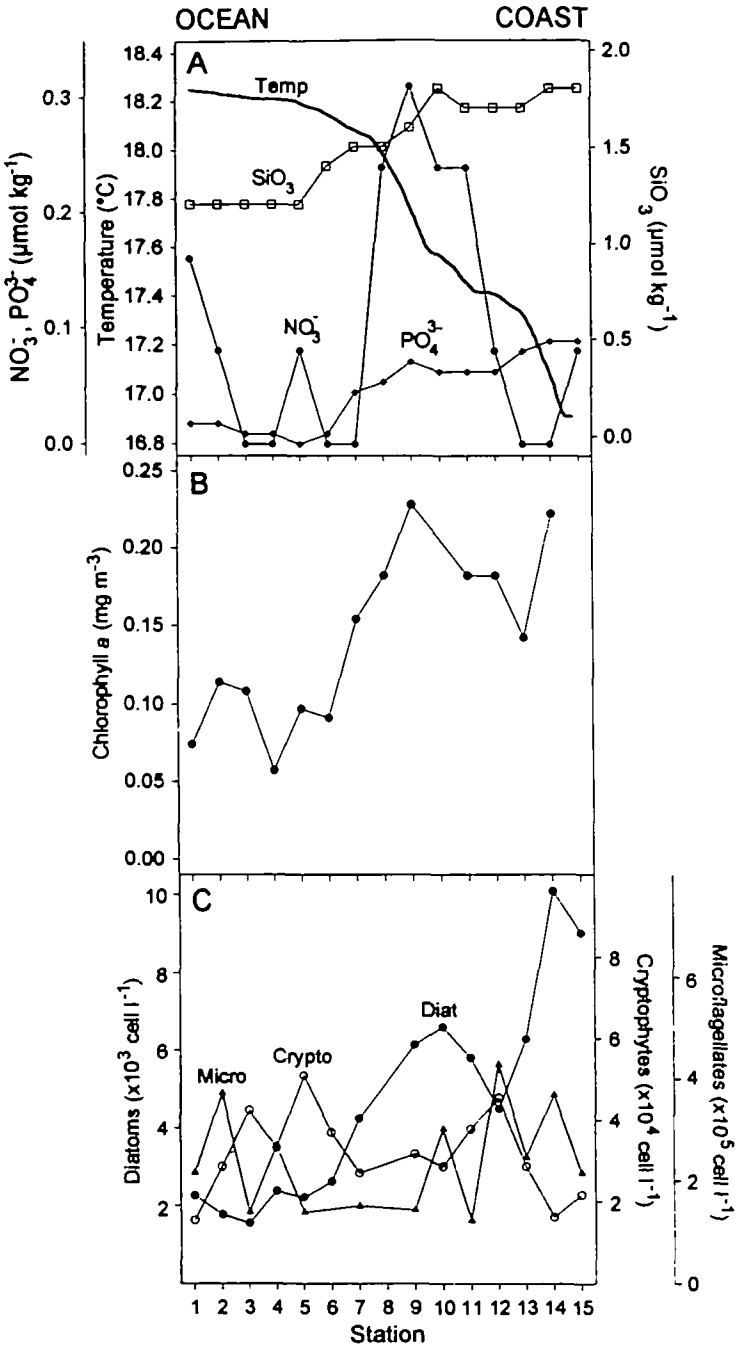

Fig. 3. Distribution of surface (2–3 m) (**A**) temperature (Temp, °C, ———), nitrate (NO_3^-, ●), phosphate(PO_4^{3-}, ♦) and silicate (SiO_3, □) concentration (µmol kg $^{-1}$), (**B**) chlorophyll *a* concentration (mg m^{-3}) and (**C**) abundance of diatoms (Diat, 10^3 cells l^{-1}, ●), cryptophytes (Crypto, 10^4 cells l^{-1}, ○) and microflagellates (Micro, 10^5 cells l^{-1}, ▲) along the transect.

The vertical distribution of chlorophyll *a* was characterized by the existence of a subsurface maximum at 20–30 m depth, where concentrations around 1.5–2.0 mg m^{-3} were measured (Figure 1C). The layer of relatively high chlorophyll *a* levels was shallower in the nearshore stations, paralleling the distribution of temperature and nitrate. Accordingly, the subsurface chlorophyll *a* maximum (~1.2 mg m^{-3}) was located at 30 m depth at station B, whereas at station A it extended from 20 to 30 m depth (Figure 2B). Integrated chlorophyll *a* concentration in the upper 40 m was 35.9 mg m^{-2} at station A, compared with 21.5 mg m^{-2} at station B. Surface chlorophyll *a* concentration increased from ~0.1 mg m^{-3} at the oceanic side of the front to values >~0.2 mg m^{-3} in the inner part of the transect (Figure 3B).

Small flagellates (~10 μm in diameter) belonging to the class Cryptophyceae and very small (~3–4 μm in diameter) unidentified microflagellates were the most abundant phytoplankters throughout this study. *Nitzschia longissima* (Brébisson) Ralfs and *Nitzschia closterium* (Ehrenberg) W. Smith accounted for >90% of total diatom number in all the samples. Clear differences in the relative importance of cryptophytes and diatoms were observed between stations A and B (data not shown). At station A, diatom abundance was in the range 2–6 × 10^3 cells l^{-1}, whereas cryptophyte numbers were <0.3 × 10^4 cells l^{-1}. In contrast, the abundance of diatoms at station B was much lower, ranging from 0.1 to 0.7 × 10^3 cells l^{-1}, and cryptophyte numbers were higher (1–1.5 × 10^4 cells l^{-1}).

The abundance of cryptophytes and microflagellates did not show any clear distributional pattern along the surface transect (Figure 3C). In contrast, the distribution of diatom density was very similar to that of chlorophyll *a*, with highest values (>6 × 10^3 cells l^{-1}) in the coastal side of the transect (Figure 3C). In accordance with the results from the vertical profiles, the relative contribution of cryptophytes to total microplankton biomass was higher (>50%) on the oceanic side of the front, concurring with the lowest chlorophyll *a* levels.

Vertical profiles of photosynthesis showed clear differences between stations A and B (Figure 2B). The depth of maximum photosynthesis was shallower at station A than at station B. Integrated primary production at station A (373.9 mg C m^{-2} day^{-1}) was distinctly higher than at station B (86.3 mg C m^{-2} day^{-1}). Changes in the distribution of surface photosynthetic rates across the transect mirrored those of chlorophyll *a* concentration. The rate of carbon incorporation was very low on the oceanic side of the front, increasing sharply at coastal stations, where it took values around 3.0 mg C m^{-3} day^{-1} (Figure 4A). The observed increases in primary production on the coastal side of the front and at station A were not only related to a higher phytoplankton biomass, but also to a sharp increase in the photosynthesis to chlorophyll *a* ratio (Figure 4A), which changed from 6–8 mg C Chl^{-1} day^{-1} at oceanic stations to >15 mg C mg Chl^{-1} day^{-1} in coastal waters.

A marked change in the patterns of carbon allocation into cellular compounds was found across the upwelling front (Figure 4B). The percentage of carbon incorporation into proteins increased from 40–45% at the coastal side of the front to ~60% at open-ocean stations. The distribution of the relative synthesis of lipids and LMWM followed the opposite pattern: highest values (15–20%) were measured at stations 10–15. Similar differences were observed when comparing the vertical distribution of the percentage of C incorporation into proteins at stations

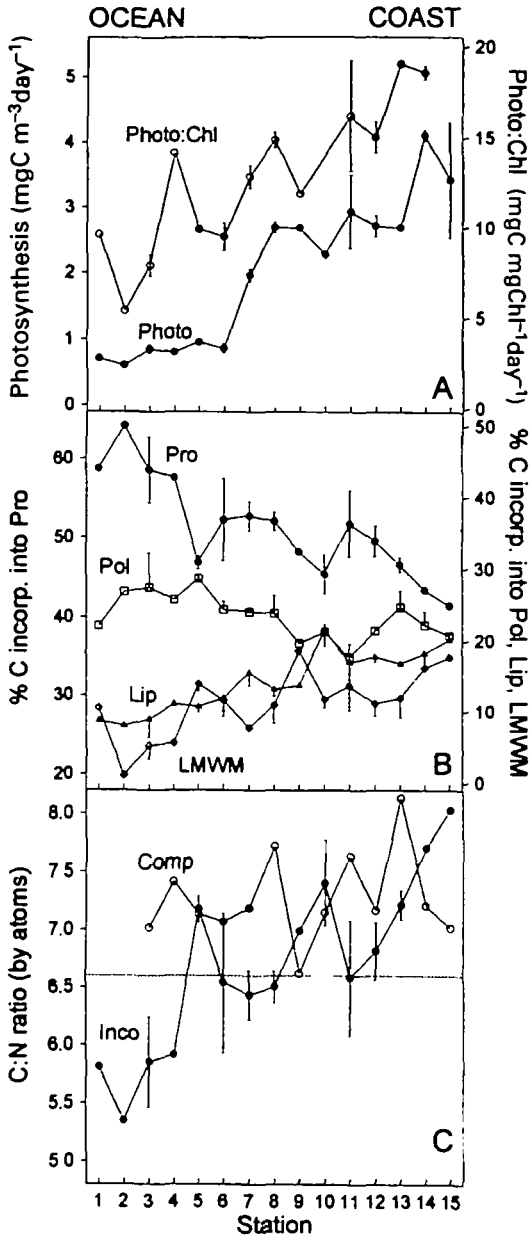

Fig. 4. Distribution of (**A**) total photosynthesis (Photo, mg C m^{-3} day^{-1}, ●) and the photosynthesis to chlorophyll *a* ratio (Photo : Chl, mg C mg Chl^{-1} day^{-1}, ○), (**B**) the percentage of carbon incorporation into proteins (Pro, ●), polysaccharides (Pol, □), lipids (Lip, ▲) and low-molecular-weight metabolites (LMWM, ◸) and (**C**) the incorporation (Inco, ●) and compositional (Comp, ○) C:N molar ratios along the surface transect. Note differences between both *y*-axes in (**B**). The dotted line in (**C**) indicates the Redfield ratio (6.6). Vertical bars represent ± 1 SE.

A and B (Figure 2C). Average relative synthesis of protein was 50.1 ± 4.7 at station B, whereas it was 40.8 ± 2.7 at station A.

As a consequence of the differences in the patterns of ^{14}C labelling, the estimated C:N uptake ratio changed conspicuously between both sides of the front (Figure 4C), higher values (>7.5) being measured at the coastal stations. A significant positive correlation was found between diatom abundance and the C:N uptake ratio ($r^2 = 0.71$, $n = 14$, $P < 0.01$). Differences in the calculated C:N ratio between coastal (stations 12–15) and oceanic (stations 1–4) samples were highly significant (ANOVA, $P = 0.0013$). In contrast, the compositional C:N ratio did not show large variations across the front, and ranged between 7.0 and 7.5 throughout the transect (Figure 4C).

Comparison of physical, chemical and biological parameters between both sides of the front suggests that the phytoplankton community inhabiting coastal waters was in an earlier successional stage. Diatoms dominated the nearshore stations, whilst the relative abundance of cryptophytes was higher in the oceanic, non-upwelled waters, where nutrient depletion had probably lasted for a longer period. This pattern agrees with the fact that small, motile cells are more efficient nutrient consumers than non-motile, large-sized algae (Geider *et al.*, 1986; Kiørboe, 1993). On the other hand, larger cells such as diatoms are known to grow faster under nutrient-sufficient conditions (Furnas, 1990). This has been related to a greater capacity for nutrient storage, which would allow diatoms to maintain relatively high growth rates after nutrient depletion (Goldman *et al.*, 1992), and also to the presence of the vacuole, which would increase the effective surface to biomass ratio. The conspicuous increase in chlorophyll *a*-normalized photosynthesis at coastal stations (Figure 4A), together with a shift in the patterns of C allocation among biomolecules (Figure 4B, see below), strongly support the view that the observed changes in the taxonomic composition were related to the different cellular physiology of each phytoplankton group.

The relative C incorporation into protein was high (~60%) in non-upwelled waters, and decreased in the coastal side of the front (Figure 4B). These observations are in agreement with those of Priscu and Priscu (1984), who found reduced levels of C incorporation into protein in the productive waters associated with the centre of another coastal upwelling. Our results are also coincident with the findings of Barlow (1984), who measured high levels of protein synthesis when nutrient concentrations decreased after an upwelling event, and those of Marañón *et al.* (1995), who reported a maintenance of protein synthesis in non-growing phytoplankton enclosed in microcosms. In addition, this metabolic strategy has previously been found in small-sized microalgae under a variety of conditions (de Madariaga and Fernández, 1990; de Madariaga and Joint, 1994), and is in accordance with the increased relative contribution of small flagellates to total phytoplankton biomass on the oceanic side of the front. Therefore, the high levels of relative protein synthesis in offshore, non-upwelled waters were probably a result of both physiological and taxonomic changes in the phytoplankton assemblages. It is well known that proteins are essential for the maintenance of basic cellular processes. Hence, the inverse correlation between relative protein synthesis and both total C incorporation and the photosynthesis to chlorophyll *a* ratio leads us to

conclude that phytoplankton cells in non-upwelled waters were adapted to low nutrient conditions by maintaining the synthesis of proteins rather than the synthesis of storage compounds.

A 2-fold increase in the relative C incorporation into lipids took place at the coastal stations (Figure 4B). It is likely that phytoplankton in the coastal region of the transect had recently been exposed to high light and nutrient conditions as a result of upwelling. The availability of an energy excess would then explain an enhanced synthesis of storage compounds, such as lipids, in the coastal waters affected by upwelling. This could also result in higher levels of particulate lipids associated with the front, as has previously been reported for other frontal processes (Gérin and Goutx, 1994).

The measurement of ^{14}C incorporation into the protein fraction allowed us to estimate the amount of N incorporation and then to calculate the C:N uptake ratio. The method used assumes a constant amino acid-N to protein-N ratio of 0.05. Nitrogen uptake computed in this way may be underestimated if a substantial proportion of N is incorporated into non-protein compounds (i.e. amino acids) or stored as internal nitrate. However, cellular accumulation of amino acids and unassimilated nitrate is very low (<5% of total N content) when cells are living in N-deficient conditions (Dortch, 1982; Dortch *et al.*, 1984). Taking into account the low levels of nitrate and ammonium measured along the surface transect, it is unlikely that the C:N ratios in Figure 4C had been significantly overestimated.

The increased C:N uptake ratios measured at the innermost stations clearly exceeded the molar Redfield ratio of 6.6. Similar results have been found by Sambrotto *et al.* (1993) studying the relationships between dissolved inorganic C and nitrate during time series in coastal and open-ocean sites. The use of the Redfield C:N ratio would then lead to a significant underestimation of the organic C production when extrapolating from nitrate consumption. As Williams *et al.* (1989) pointed out, the ratio of exported C to nitrate import in the euphotic layer is dependent, in the long term, on the variability of hydrodynamic forcing. Our results show that the physiological response of phytoplankton to upwelling may result in an increase in the C:N consumption ratio. If these findings prove to be valid over extended spatial and temporal scales, then upwelling may represent a mechanism whereby physical forcing brings about a synthesis of organic C higher than predicted from the upward flux of nitrate and the Redfield ratio.

Acknowledgements

This research was funded by the Spanish CICYT contract AMB 92-0834. The authors wish to thank A.Botas and J.A.Sostres for providing nutrient data, R.González-Quirós for assistance during field work, and P.Serret and R.Anadón for help at the laboratory. E.M. acknowledges the receipt of a PFPI fellowship from the Spanish Ministry of Science and Education.

References

Barlow,R.G. (1984) Dynamics of the decline of a phytoplankton bloom after an upwelling event. *Mar. Ecol. Prog. Ser.*, **16**, 121–126.

de Madariaga,I. and Fernández,E. (1990) Photosynthetic carbon metabolism of size-fractionated phytoplankton during an experimental bloom in marine microcosms. *J. Mar. Biol. Assoc. UK*, **70**, 531–543.

de Madariaga,I. and Joint,I.R. (1994) Photosynthesis and carbon metabolism by size-fractionated phytoplankton in the southern North Sea in early summer. *Cont. Shelf Res.*, **14**, 295–311.
DiTullio,G.R. and Laws,E.A. (1983) Estimates of phytoplankton N uptake based on $^{14}CO_2$ incorporation into protein. *Limnol. Oceanogr.*, **28**, 177–185.
Dortch,Q. (1982) Effect of growth conditions on accumulation of internal nitrate, ammonium, amino acids and protein in three marine diatoms. *J Exp. Mar. Biol. Ecol.*, **61**, 243–264.
Dortch,Q., Clayton,J.R., Thoresen,S.S. and Ahmed,S.I. (1984) Species differences in accumulation of nitrogen pools in phytoplankton. *Mar Biol.*, **81**, 237–250.
Fernández,E., Balch,W.M., Marañón,E. and Holligan,P.M. (1994) High rates of lipid biosynthesis in cultured, mesocosm and coastal populations of the coccolithophore *Emiliania huxleyi*. *Mar. Ecol. Prog. Ser.*, **114**, 13–22.
Fraga,F. and Pérez,F.F. (1990). Transformaciones entre composición química del fitoplancton, composición elemental y relación de Redfield. *Sci. Mar* **54**, 69–76.
Furnas,M.J. (1990) *In situ* growth rates of marine phytoplankton: approaches to measurement, community and species growth rates. *J. Plankton Res.*, **12**, 1117–1151.
Geider,R.J., Platt,T. and Raven,J.A. (1986) Size dependence of growth and photosynthesis in diatoms: a synthesis. *Mar. Ecol. Prog. Ser.*, **30**, 93–104.
Gérin,C. and Goutx,M. (1994) Latroscan measured particulate and dissolved lipids in the Almeria-Oran frontal system (Almofront-1, May 1991). *J. Mar. Systems*, **5**, 343–360.
Goldman,J.C., Hansell,D.A. and Dennett,M.R. (1992) Chemical characterization of three large oceanic diatoms: potential impact on water column chemistry. *Mar. Ecol. Prog. Ser.*, **88**, 257–270.
Holligan,P.M., Harris,R.P., Newell,R.C., Harbour,D.S., Linley,E.A.S., Lucas,M.I., Tranter,P.R.G. and Weekley,C.M. (1984) Vertical distribution and partitioning of organic carbon in mixed, frontal and stratified waters of the English Channel. *Mar. Ecol. Prog. Ser.*, **14**, 111–127.
Kiørboe,T. (1993) Turbulence, phytoplankton cell size, and the structure of pelagic food webs. *Adv. Mar. Biol.*, **29**, 1–72.
Laws,E.A. (1991) Photosynthetic quotients, new production and net community production in the open ocean. *Deep-Sea Res.*, **38**, 143–167.
Marañón,E., Fernández,E. and Anadón,R. (1995) Patterns of macromolecular synthesis by natural phytoplankton assemblages under changing upwelling regimes: *in situ* observations and microcosms experiments. *J. Exp. Mar. Biol. Ecol.*, **188**, 1–28.
Priscu,J.C. and Priscu,L.R. (1984) Photosynthate partitioning by phytoplankton in a New Zealand coastal upwelling system. *Mar. Biol.*, **81**, 31–40.
Sambrotto,R.N., Savidge,G., Robinson,C., Boyd,P., Takahashi,T., Karl,D.M., Langdom,C., Chipman,D., Marra,J. and Codsipoti,L. (1993) Elevated consumption of carbon relative to nitrogen in the surface ocean. *Nature*, **363**, 248–250.
Wilkerson,F.P. and Dugdale,R.C. (1987) The use of large shipboard barrels and drifters to study the effects of coastal upwelling on phytoplankton dynamics. *Limnol. Oceanogr.*, **32**, 368–382.
Williams,P.J.leB., von Bodungen,B., Bathman,U., Berger,W.H., Eppley,R.W., Feldman,G.C., Fischer,G.C., Legendre,L., Minster,J.-F., Reynolds,C.S., Smetacek,V.S. and Toggweiler,J.R. (1989) Export productivity from the photic zone. In Berger,W.H., Smetacek,V.S. and Wefer,G. (eds), *Productivity of the Ocean: Present and Past*. John Wiley and Sons, Chichester, pp. 99–115.
Zimmerman,R.C., Kremer,J.N. and Dugdale,R.C. (1987) Acceleration of nutrient uptake by phytoplankton in a coastal upwelling ecosystem: A modelling analysis. *Limnol. Oceanogr.*, **32**, 359–367.

Received on March 19, 1995; accepted on June 1, 1995